

Covering-Space Normalizing Flows: Approximating Pushforwards on Lens Spaces

William Ghanem

Department of Mathematics, University of Texas at Austin

December 1, 2025

Abstract

We construct pushforward distributions via the universal covering map $\rho : S^3 \rightarrow L(p; q)$ with the goal of approximating these distributions using flows on $L(p; q)$. We highlight that our method deletes redundancies in the case of a symmetric S^3 distribution. Using our model, we approximate the pushforwards of von Mises–Fisher–induced target densities as well as that of a \mathbb{Z}_{12} -symmetric Boltzmann distribution on S^3 constructed to model Benzene.

1 Introduction

Normalizing flows provide a family of invertible generative transformations that enable the approximation of complex probability distributions [1]. While they are simpler to admit on Euclidean spaces, many works have extended the implementation to general manifolds. For instance, Rezende *et al.* successfully modeled flows on Tori and Spheres [2]. Katsman *et al.* introduced a method for learning flows on the intrinsic manifold by enforcing both an equivariant prior and equivariant transformations [3]. As their experiments suggest, the method is both elegant and robust. That said, their method deals with smooth actions; many quotient manifolds are obtained through covering spaces, where discrete actions must be addressed. In our paper, we construct the pushforward of an S^3 distribution onto $L(p; q)$ using the universal covering map $\rho : S^3 \rightarrow L(p; q)$ and approximate such distributions using a flow on $L(p; q)$. We observe the appealing property that our construction removes distribution symmetries in S^3 with respect to the covering space deck transformations by passing to the quotient. In particular, with a careful choice of base space parameterization, simple flows can accurately approximate pushforward distributions on these manifolds in a computationally inexpensive way. Our method leverages the **Heegaard decomposition** of $L(p; q)$, which essentially reduces the problem’s dimensional complexity by viewing $L(p; q)$ as a boundary quotient of two solid tori - domains on which flow construction is considerably simpler. To motivate the approach, we apply our model to Benzene, using an associated Boltzmann distribution to demonstrate its use in context of molecules with symmetries.

Why Lens Spaces

Lens spaces are 3-dimensional manifolds obtained as quotients of the 3-sphere under a \mathbb{Z}_p action (see background). While they are topologically complex, they admit a tractable decomposition into two solid tori, in which we may extract parameterizations which are great to test manifold flows on.

Beyond their mathematical appeal, lens spaces arise naturally in molecular dynamics. The energy configuration space of a rigid molecule acted on by rotations is $SO(3)$, which is diffeomorphic to $L(2; 1)$. Lifting to the universal cover, Karney showed in [4] that the configuration space may be viewed as S^3 , introducing a \mathbb{Z}_2 redundancy. At first glance, this lift seems to move away from lens spaces. However, it actually clarifies how more general lens spaces emerge: if a molecule exhibits a p -fold rotational energy symmetry in the $SO(3)$ configuration space, these redundancies can be modded out, yielding the quotient $S^3/\mathbb{Z}_{2p} \cong L(2p, 1)$. A simple example is a cyclic carbon molecule such as benzene, which possesses $p = 6$ rotational symmetry.

2 Background

2.1 Normalizing Flows

In normalizing flows, we have two probability spaces (Z, μ_Z) and (X, μ_X) where Z and X are the same manifold, μ_Z is the base prior distribution, and μ_X is the target distribution. The objective is to train a diffeomorphism $F_\theta : Z \rightarrow X$ (θ being a finite list of trainable parameters) such that the pushforward distribution of the prior approximates the target, that is, $F_{\theta*}\mu_Z \approx \mu_X$. The metric we use to achieve this approximation is the KL divergence between the PDF of the pushforward $F_{\theta*}\mu_Z$ and the PDF of μ_X . By the change of variable formula, $F_{\theta*}\mu_Z$ has PDF

$$q(x) = p_Z(F_\theta^{-1}(x)) \left| \det J_{F_\theta^{-1}}(x) \right|$$

and so the KL divergence between $F_{\theta*}\mu_Z$ and μ_X is given by

$$\text{KL}(F_{\theta*}\mu_Z|\mu_X) = \mathbb{E}_{x \sim F_{\theta*}\mu_Z} \left[\log \frac{q(x)}{p_X(x)} \right] = \int_X q(x) \log \frac{q(x)}{p_X(x)} dx$$

In practice, we approximate the above via MC sampling on the equivalent expectation formula

$$\text{KL}(F_{\theta*}\mu_Z|\mu_X) = \mathbb{E}_{z \sim \mu_Z} [\log(p_Z(z)) - \log(|\det J_{F_\theta}(z)|) - \log(p_X(F_\theta(z)))]$$

Hence, by training the diffeomorphism F_θ with respect to the parameters θ by minimizing the expectation formula above, we may learn sampling the target μ_X by sampling first the prior μ_Z and, afterwards, applying F_θ .

2.2 Lens Spaces and Heegaard Splittings

The manifold $L(p; q)$ is obtained as a quotient of $S^3 \subset \mathbb{C}^2$ by the \mathbb{Z}_p action generated by $(z_1, z_2) \mapsto (e^{\frac{2\pi i}{p}}, e^{\frac{2\pi i q}{p}})$. We assume always that $\gcd(p, q) = 1$. The action is free, and since S^3

is simply connected, the quotient map $\rho : S^3 \rightarrow L(p; q)$ corresponds to the universal cover of $L(p; q)$.

One may also define $L(p; q)$ by their genus 1 Heegaard splitting. First, we provide a formal definition of a genus g Heegaard splitting.

Definition 1. *A **genus g Heegaard splitting** of a 3-manifold M is a triple (V_1, V_2, f) such that each V_i is a genus g handlebody, $f : \partial V_1 \rightarrow \partial V_2$ is a homeomorphism of the bounding genus g surfaces of V_1 and V_2 , and the quotient manifold $V_1 \cup_f V_2$ is homeomorphic to M .*

In the definition above, $V_1 \cup_f V_2$ refers to the quotient of $V_1 \cup V_2$ that identifies $v \in \partial V_1$ with $f(v) \in \partial V_2$.

In the context of $L(p; q)$, we locate the genus 1 handlebodies explicitly. Indeed, consider the universal cover S^3 as a submanifold of \mathbb{C}^2 , we set $U_i = \{|z_i|^2 \leq \frac{1}{2}\}$, $i=1,2$. Under the universal cover $\rho : S^3 \rightarrow L(p; q)$, we set $V_i = \rho(U_i)$. We construct diffeomorphisms $S^1 \times D^2 \rightarrow V_i$ as follows:

$$f_1 : S^1 \times D^2 \rightarrow V_1$$

$$f_1(e^{i\theta}, \rho e^{i\phi}) = \left[\left(\sqrt{\frac{1}{2}} \rho \cdot e^{i(\phi + \frac{r}{p}\theta)}, \sqrt{1 - \frac{1}{2}\rho^2} \cdot e^{i\frac{\theta}{p}} \right) \right]$$

and, for V_2

$$f_2 : S^1 \times D^2 \rightarrow V_2$$

$$f_2(e^{i\theta}, \rho e^{i\phi}) = \left[\left(\sqrt{1 - \frac{1}{2}\rho^2} \cdot e^{i\frac{\theta}{p}}, \sqrt{\frac{1}{2}} \rho \cdot e^{i(-\phi + \frac{q}{p}\theta)} \right) \right]$$

Note that the square brackets indicate that we are in the quotient manifold, hence the outputs consist of equivalence classes under the action of S^3 . Furthermore, $r = q^{-1} \bmod p$. Let $A = \begin{pmatrix} r & p \\ s & q \end{pmatrix}$ where $s = \frac{rq-1}{p}$. It is easy to verify that $f_1|_{S^1 \times S^1} = f_2|_{S^1 \times S^1} A$ (where A is

applied to the tuple $\begin{pmatrix} \theta \\ \phi \end{pmatrix}$), hence A provides the gluing map that we refer to in the Heegaard splitting definition. Indeed, if we let $T_i = \text{domain}(f_i)$ then $T_1 \cup_A T_2 \cong L(p; q)$ via the map $f_1 \cup_A f_2$. Note that $f_1 \cup_A f_2$ is defined as $f_1 \cup_A f_2(x) = f_i(x)$ if $x \in T_i$. If $x \in T_1 \cap T_2$, the point is that $f_1(x) = f_2(x)$ in the quotient topology induced by the gluing map A , so the map is well defined. Hence, $T_1 \cup_A T_2$ provides a Heegaard splitting of $L(p; q)$.

3 Method

3.1 Pushforward from S^3

We provide a tractable method of constructing the pushforward of a distribution on S^3 onto $L(p; q)$. In order to achieve this, we work in the Heegaard splitting of $L(p; q)$ from 2.2, so we view this pushforward distribution as living on $T_1 \cup_A T_2$ via the global diffeomorphism defined by $f_1 \cup_A f_2$. For a detailed construction see the appendix A.1.

We have a distribution μ_{S^3} on S^3 with pdf p_{S^3} with respect to the Riemannian volume metric. If p_{S^3} is not already symmetric with respect to the action on S^3 we construct the symmetrized pdf $p_{sym}(x) = \frac{1}{n} \sum_i^n p_{S^3}(gx)$ and we denote its distribution by μ_{sym} . Here, the action by elements g is encoded lens space action defined in 2.2. Using Proposition 3 (see A.1), we know that $\rho_*\mu_{S^3} = \rho_*\mu_{sym}$, so it suffices to work with the symmetrized distribution (if the pdf is already symmetric, $p_{sym} = p_{S^3}$ and there is no use in symmetrizing again). Pushing the symmetrized distribution to $T_1 \cup_A T_2$, we obtain the formula $p_1 \cup_A p_2 = \frac{1}{2} p_{sym} \circ \psi \circ h_i^{-1}(e^{i\theta}, x, y)$ for $(e^{i\theta}, x, y) \in T_i$ where $\psi : S^3 \subset \mathbb{C}^2 \rightarrow S^3 \subset \mathbb{R}^4$ is the typical map converting \mathbb{C}^2 coordinates to cartesian, $h^{-1} : S^1 \setminus \{1\} \times D^2 \subset T_i \rightarrow S^3$ is exactly the map f_i defined in 2.2 but lifted to S^3 by removing the square brackets, and $\frac{1}{2}$ comes from pulling the Riemannian volume element on S^3 to $T_1 \cup_A T_2$. Implicitly, we are converting (x, y) to polar before applying h_i^{-1} , so that $p_1 \cup_A p_2$ is a density with respect to $d\theta dx dy$. Another note is that is that, while h_i^{-1} is not defined on all of T_i , p_i is since p_{sym} is symmetric and h_i^{-1} is well defined on fibers of $\rho : S^3 \rightarrow L(p; q)$. By construction, $p_1 \cup_A p_2$ is the density of the desired distribution on $T_1 \cup_A T_2$ with respect to the Lebesgue measure on $S^1 \times D^2$ that satisfies the same local properties as p_{S^3} (eg. continuity, smoothness). At the boundary of T_1 , these local properties are still satisfied via the gluing map A .

In practice, we train independently on each T_i , so we conveniently normalize each p_i by their integral in T_i to obtain two final training pdfs $q_i = \frac{1}{I_i} p_i$ defined on T_i , where I_i is the MC approximation of $\int_{S^1 \times D^2} p_i d\theta dx dy$. In terms of the q_i the final pdf on $T_1 \cup_A T_2$ is given by $q(a) = I_1 q_1 \cup_A I_2 q_2(a) = I_i q_i(a)$ if $a = (e^{i\theta}, x, y) \in T_i$. Hence, if we define the following random variables

$$X_i \sim q_i$$

$$X \sim q \text{ (the target)}$$

and let $X_B \sim \text{Bernoulli}(I_2)$, then

$$X = (1 - X_B)X_1 + X_B X_2$$

and so approximating the $X_i \sim q_i$ provides an approximation for X .

3.2 Architecture and Training Methods

Training Architecture

As mentioned briefly in 3.1, we train on each tori T_i separately with target q_i . We use a method involving coupling layers, inspired by the construction in [5]. A trainable map on a torus is constructed as a sequence of coupling layers, with each coupling layer a function $\mathbb{R}^3 \rightarrow \mathbb{R}^3$. We use two different types of coupling layers: one that fixes the coordinate corresponding to S^1 while changing the coordinates corresponding to D^2 , and another, which fixes the coordinates corresponding to D^2 while fixing the coordinate corresponding to S^1 . Each coupling layers consists of two trainable linear neural networks s_i and t_i (scale and translate). The first coordinate of \mathbb{R}^3 corresponds to S^1 , and at the end of a sequence of coupling layers it is wrapped back to $[0, 2\pi)$ by taking the modulus. The last two correspond D^2 . We map the interior of D^2 diffeomorphically to \mathbb{R}^2 , apply the coupling layers to these

coordinates, then revert back to D^2 via the inverse diffeomorphism. For a more formal description see A.2.

Prior Distribution

We give our choice of prior distribution defined on $Z_i = S^1 \times D^2$. We use $\mu_{Z_i} \sim VM_{[0,2\pi)}(0, \kappa_i) \times N(0, \sigma_i^2 I_2)|_{D^2}$. In plain english, for the S^1 product, we use a von Mises distribution in $[0, 2\pi)$ centered at 0 with concentration κ_i and in the D^2 product, we use a truncated normal distribution centered at the origin with variance σ_i^2 . Its pdf is given by:

$$p_{Z_i}(\theta, x, y) = \frac{1}{2\pi I_0(\kappa_i)} e^{\kappa_i \cos(\theta)} \cdot \frac{1}{2\pi\sigma_i^2(1 - e^{-1/(2\sigma_i^2)})} e^{-\frac{x^2+y^2}{2\sigma_i^2}}$$

for $(\theta, x, y) \in [0, 2\pi) \times D^2$.

Training

Given all the above, training $F_{\theta_i} : Z_i \rightarrow T_i$ is straightforward: (1) sample the prior on Z_i , (2) approximate the KL divergence between the prior pushforward through F_{θ_i} and the target on T_i using F_{θ_i} applied to the samples, and (3) train the parameters θ_i of F_{θ_i} using Adam optimizer with KL divergence as a loss function. Additionally, we anneal an additional Shannon entropy term over the first several epochs to increase early exploration.

4 Experiments

We conduct three experiments in total: the first two using linear combinations of von Mises-Fisher (vMF) distributions with varying modes and the third using a Boltzmann distribution on S^3 .

vMF Experiments

The vMF(μ, κ) pdf is given by

$$f(x; \mu, \kappa) = \frac{\kappa}{4\pi^2 I_1(\kappa)} e^{\kappa \mu \cdot x}$$

and is a density with respect to $d\text{vol}_{S^3}$. For the first experiment, we are in the setting $\rho : S^3 \rightarrow L(3; 2)$. We use as S^3 distribution

$$p_{S^3}^1(x) = \frac{1}{2} \left(\frac{1}{2} (f(x; c_1, 35) + f(x; c_2, 35)) + \frac{1}{3} (f(x; b_1, 35) + f(x; b_2, 35) + f(x; b_3, 35)) \right)$$

where

$$\begin{aligned} c_1 &= (1, 0, 0, 0), \quad c_2 = (\cos(\pi/3), \sin(\pi/3), 0, 0) \\ b_1 &= (0, 0, 1, 0), \quad b_2 = (0, 0, \cos(\pi/4), \sin(\pi/4)), \quad b_3 = (0, 0, \cos(\pi/2), \sin(\pi/2)) \end{aligned}$$

This pdf has 5 modes (3 in U_1 and 2 in U_2) each lying in the same fundamental domain, and so the symmetrized pdf will have 15 modes (9 in U_1 and 6 in U_2). In Figure 1, we see that we get the expected 3 modes in T_1 and 2 modes in T_2 . Recall from 3.1 that we work with the symmetrized pdf, regardless of whether the original S^3 distribution is symmetric or not. The number of modes in Figure 1 therefore qualitatively demonstrates the symmetry deletion feature if we consider $p_{S^3}^1$ as being its symmetrized pdf.

As a second experiment, we use a more difficult density function. Here, we are in the setting $\rho : S^3 \rightarrow L(7; 3)$

$$p_{S^3}^2(x) = \frac{1}{3} \left(\frac{1}{3}(f(x; c_1, 65) + \frac{2}{3}f(x; c_2, 55)) \right) + \frac{2}{3} \left(\frac{2}{3}(f(x; b_1, 65) + \frac{1}{3}f(x; b_2, 80)) \right)$$

where

$$\begin{aligned} c_1 &= (\sqrt{\frac{2}{3}}, 0, \sqrt{\frac{1}{3}}, 0), \quad c_2 = (\sqrt{\frac{3}{4}} \cos(\pi/7), \sqrt{\frac{3}{4}} \sin(\pi/7), \sqrt{\frac{1}{4}}, 0) \\ b_1 &= (0, \sqrt{\frac{1}{4}}, \sqrt{\frac{3}{4}}, 0), \quad b_2 = (\sqrt{\frac{1}{7}}, \sqrt{\frac{1}{7}}, \sqrt{\frac{5}{7}} \cos(4\pi/21), \sqrt{\frac{5}{7}} \sin(4\pi/21)) \end{aligned}$$

This pdf has 4 modes (2 in both U_1 and U_2) each lying in the same fundamental domain. Hence, the symmetrized pdf has 28 modes (14 in both U_1 and U_2). As in the first experiment, these symmetries are deleted and we get the expected 2 modes in both T_1 and T_2 (see Figure 1).

Boltzmann Experiment

We train on the pushforward of an S^3 Boltzmann distribution for Benzene given by $p_{S^3}^{Boltz}(q) = \frac{1}{C} e^{U(q; 5, e_1, 20, e_1, e_2)}$, where

$$U(q; \kappa, c, V, x_0, y_0) = -\kappa(n(q; x_0) \cdot c)^2 + (n(q; x_0) \cdot c)^2 V(1 - \cos(6\phi(q; y_0)))$$

The first term is a Maier-Saupe potential term [6] and the second is a 6-fold Hindered Rotor potential [7]. $n(q; x_0)$ is defined as $R(q)x_0$ where $R(q)$ is the $SO(3)$ matrix corresponding to q in the double cover $S^3 \rightarrow SO(3)$ and $\phi(q; y_0)$ is defined by projecting $R(q)y_0$ onto the normal plane of c and then computing a rotation angle using the arctan of coordinates in this normal plane via a preselected orthonormal basis (see A.4). Using $c = e_1$, as is done in $p_{S^3}^{Boltz}$, U is invariant under the $L(12; 1)$ deck action on S^3 and so $p_{S^3}^{Boltz}$ is symmetric. Hence, this experiment directly addresses the second paragraph of “Why Lens Spaces” - we intend on modding out energy symmetries of U . Specifically, with our chosen hyperparameters, we expect there to be a total of 24 modes in S^3 . In $T_1 \cup_A T_2 \cong L(12; 1)$, we expect 2 modes - one in each solid torus T_i . We see in Figure 1 that we achieve exactly this.

Results

Table 1 reports KL values across the three target distributions denoted 1,2, and Boltz. In A.3, we derive a relationship between global KL and local KL values. Given that the constants I_2 for each experiment are $\approx 0.5, 0.3, 0.5$ (1,2, and Boltz respectively), Table 1 shows the KL values computed via global sampling (the values in row Flow- $L(p; q)$) and the ones computed via equations A.3 using local estimates (the first two rows of Table 1) agree within 0.01 nats.

KL (nats)	1	2	Boltz
Flow- T_1	0.10 ± 0.01	0.24 ± 0.03	0.22 ± 0.03
Flow- T_2	0.12 ± 0.01	0.12 ± 0.01	0.25 ± 0.02
Flow- $L(p; q)$	0.11 ± 0.01	0.20 ± 0.02	0.24 ± 0.02

Table 1: KL values for the model applied to pushforwards of $p_{S_3}^1$ (left), $p_{S_3}^2$ (middle), and $p_{S^3}^{Boltz}$ (right). Trained using prior parameters $\sigma_i = 0.25$, $\kappa_i = 5$, $i = 1, 2$. Results averages over 5 seeds within one standard deviation. Sample sizes on each T_i were 6000. Initial total KL values ranged from 5-15 nats.

Qualitative

We include visuals that emphasize the modes in each of the approximations, shown in Figure 1. For each experiment, denoted 1, 2, and Boltz, we take 100,000 samples and keep only samples within the 99th percentile of pushforward pdf evaluations on each T_i . We separate our observations into two types: global (observations that compare T_1 and T_2 .) and local (those that are made within a particular T_i).

Global: In 1 and Boltz, we see similar sampling frequency in both T_1 and T_2 . In 2, T_1 captures a larger number of samples, a behavior captured by the sample density associated to the bottom left mode of T_1 (which is the mode associated to b_1). Conversely, both modes in T_2 appear less dense. Furthermore, in 2, there is a clear distinction between the pdf evaluations associated to modes on T_1 and T_2 - the modes in T_1 are yellow (indicating a larger pdf evaluation), whereas the modes in T_2 are red. In 1, the modes are slightly higher in T_2 , and in Boltz, they have similar coloring.

Local: In 1, the modes for each of the T_i appear identical. In 2, the mode associated to b_1 is heavily sampled and encapsulates a larger surface area compared to the mode associated to b_2 , which is faintly visible in the back of T_1 . Still in 2, the mode in the right corner of T_2 (associated to c_2) is sampled more than the left corner mode (associated to c_2) and encapsulates a larger surface area. In Boltz, each T_i has just one mode and the symmetric nature of the density across the T_i allows pure a clearer modal structure - the center of the neighborhoods are more yellow face into red.

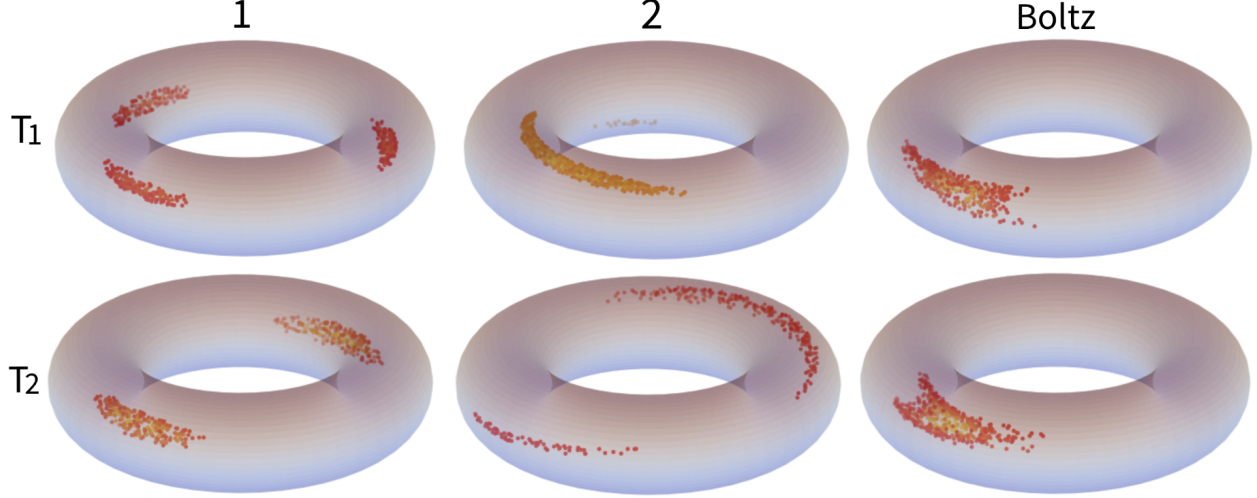


Figure 1: Samples from the the learned distribution on $T_1 \cup_A T_2$ associated to the pushforwards of $p_{S^3}^1$ (left), $p_{S^3}^2$ (middle), and $p_{S^3}^{Boltz}$ (right) visualized on each T_i . Only samples within the top 1% of pushforward pdf values are shown to highlight the high density regions. Higher density is in yellow, lower density is red.

5 Discussion

Our model learns pushforward distributions of the covering map $\rho : S^3 \rightarrow L(p; q)$ by constructing flows on each Heegaard solid torus and training against the target, achieving small KL values in experiments. By construction, the pushforward distribution on $L(p; q)$ satisfies all local properties as that on S^3 , and these properties on the boundary of T_1 are encoded by the gluing map in 2.2. In particular, in the case of smooth distributions that exhibit symmetries, we may mod out these symmetries and learn the pushforward distribution on a lens space, which remains smooth and retains the relevant probabilistic information. This allows for learning a distribution with simpler properties; in this paper, we focused on the reduction of modes. The caveat is adding topological complexity and working on a more complicated manifold, but this is controlled by using the Heegaard decomposition as a way to parametrize. In the experiments conducted, we observe the concept of symmetry deletion by sampling the modes of the learned distribution. The observed local and global properties are consistent with the chosen targets, demonstrating accurate learning across and within both tori of the Heegaard decomposition. As a final experiment, we accurately learned the pushforward of a Boltzmann distribution on S^3 with symmetries, demonstrating the ability to simulate molecular configurations on a configuration space without the rotational redundancies.

6 Conclusion

We introduced a method for learning distributions on lens spaces using the universal cover $\rho : S^3 \rightarrow L(p; q)$ and their Heegaard decomposition. The approach achieves near zero KL divergence to pushforward targets which are smooth along the Heegaard gluing map. The

model removes quotient symmetries and can be used to learn Boltzmann distributions on the symmetry-reduced configuration space. Future work includes extending the covering space framework to other manifolds.

References

- [1] I. Kobyzev, S. J. D. Prince, and M. Brubaker. *Normalizing Flows: An Introduction and Review of Current Methods*. arXiv:1908.09257, 2020.
- [2] D. J. Rezende, S. Mohamed, et al. *Normalizing Flows on Tori and Spheres*. arXiv:2002.02428, 2020.
- [3] I. Katsman, A. Lou, D. Lim, Q. Jiang, S.-N. Lim, and C. De Sa. *Equivariant Manifold Flows*. In *Advances in Neural Information Processing Systems (NeurIPS)*, 2021.
- [4] C. F. F. Karney. *Quaternions in Molecular Modeling*. arXiv:physics/0506177, 2006.
- [5] F. Noé, S. Olsson, J. Köhler, and H. Wu. *Boltzmann Generators: Sampling Equilibrium States of Many-Body Systems with Deep Learning*. arXiv:1812.01729, 2019.
- [6] W. Maier and A. Saupe. *Eine einfache molekulare Theorie des nematischen kristallinflüssigen Zustandes*. *Zeitschrift für Naturforschung A*, 14:882–889, 1959.
- [7] K. S. Pitzer and W. D. Gwinn. *Energy Levels and Thermodynamic Functions for Molecules with Internal Rotation I*. *J. Chem. Phys.*, 10(7):428–440, 1942.

A Appendix

A.1 Construction of the Pushforward

We give a more in depth description of how we obtain smooth densities on lens spaces via pushforward distributions originating from S^3 . But first, we note that the S^3 pushforward case is complete in the sense that any distribution on $L(p; q)$ arises as the pushforward of a distribution on S^3 .

Proposition 2. *Given a finite sheeted covering map $\rho : M \rightarrow N$ and a distribution μ_N on N , there exists a distribution μ_M on M such that $\mu_N = \rho_*\mu_M$.*

Proof. Let $F \subset M$ be a fundamental domain for the cover (F necessarily exists since we are dealing with manifolds). Define a PDF on F by $p_F = p_N \circ \iota$ where $\iota = \rho|_F$ and p_N is the density of μ_N . Given $x \in M$, let h_x denote the unique deck transformation that sends x to F . Define p_M by $p_M(x) = \frac{1}{m}p_F(h_x(x))$ where m is the number of sheets. Then the distribution μ_M associated to p_M satisfies $\rho_*\mu_M = \mu_N$. \square

The sketched proof above provides the idea of how we are going to obtain the pushforward: we will work with fundamental domains. We prove another result which is necessary for our case.

Proposition 3. Let $\rho : M \rightarrow N$ be a finite sheeted covering map and μ_M be a distribution on M . Suppose μ_M has density function p_M with respect to measure m on M . Let $g_i, i=1, \dots, n$ be the deck transformations of M and define $p_{sym}(x) = \frac{1}{n} \sum_i^n p_M(g_i x)$ where n is the number of sheets. Let μ_{sym} be the distribution associated to p_{sym} . Then $\rho_* \mu_M = \rho_* \mu_{sym}$.

Proof. Let $F \subset M$ be a fundamental domain for N . Then $\rho_* \mu_M$ has pdf (with respect to $\rho_* m$) $p(y) = \sum_{i=1}^n p_M(g_i \rho|_F^{-1}(y))$. Furthermore, $\rho_* \mu_{sym}$ has pdf $p_s(y) = \sum_{i=1}^n p_{sym}(g_i \rho|_F^{-1}(y)) = \frac{1}{n} \sum_{i,j=1}^n p_M(g_j g_i \rho|_F^{-1}(y)) = \frac{1}{n} \sum_{i=1}^n n \cdot p_M(g_i \rho|_F^{-1}(y)) = p(y)$. \square

Proposition 3 applies directly to our context - $M = S^3$, $N = L(p; q)$, μ_{S^3} is some distribution on S^3 , and the measure on S^3 is $d\text{vol}_{S^3}$, which is the volume measure induced by the typical Riemannian metric on S^3 . In section 2.2, we introduced maps f_i $i = 1, 2$. If we remove the square brackets so that the image lives in $S^3 \subset \mathbb{C}^2$ and view (θ, ρ, ϕ) as elements of $[0, 2\pi) \times [0, 1] \times [0, 2\pi)$, we get fundamental domains for V_i (their union is a fundamental of $L(p; q)$). Denote these subsets of S^3 by F_i $i = 1, 2$. Then we have the following commutative diagram:

$$\begin{array}{ccc} F_1 \cup F_2 & \xrightarrow{\iota} & S^3 \subset \mathbb{C}^2 \\ \downarrow h_1 \cup h_2 & & \downarrow \rho \\ T_1 \cup_A T_2 & \xrightarrow{f_1 \cup_A f_2} & L(p; q) \end{array} \quad \begin{array}{c} \xrightarrow{\psi} \\ S^3 \subset \mathbb{R}^4 \end{array}$$

where ι is the inclusion map, $h_i = f_i^{-1} \circ \rho \circ \iota$, and $\psi : S^3 \rightarrow S^3$ is the standard map converting \mathbb{C}^2 polar coordinates to \mathbb{R}^4 cartesian coordinates. The desired target distribution is $((f_1 \cup_A f)^{-1} \circ \rho \circ \psi^{-1})_* \mu_{S^3}$, we wish to determine its pdf. Suppose μ_{S^3} has pdf p_{S^3} with respect $d\text{vol}_{S^3}$. The action on $S^3 \subset \mathbb{C}^2$ induces an action on $S^3 \subset \mathbb{R}^4$, and we symmetrize with respect to this action to get a pdf p_{sym} . For $z = (e^{i\theta}, x, y) \in V_i$, define $p_{V_i}(z) = p \cdot p_{sym} \circ \psi \circ \iota \circ h_i^{-1}(z)$ where, technically, h_i^{-1} is defined on $S^1 \setminus \{1\} \times D^2$ (note that the total composition is well defined on $S^1 \times D^2$ since p_{sym} is symmetric with respect to the action and h_i^{-1} is well defined on fibers of the covering map ρ). Also, we note that we swapped to cartesian coordinated in D^2 - in practice, we reconvert to polar then apply h_i^{-1} . Since $d\text{vol}_{S^3}$ is Haar with respect to the \mathbb{Z}_p action and p_{sym} is symmetric, the multiplication by p in the definition of p_{V_i} corresponds to summing over the \mathbb{Z}_p translates of $\iota \circ h_i^{-1}(x)$, as in the proof of Proposition 3. Hence, by commutativity of the diagram above, $p_{V_1} \cup_A p_{V_2}$ is the pdf of $((f_1 \cup_A f)^{-1} \circ \rho \circ \psi^{-1})_* \mu_{S^3}$ with respect to $((f_1 \cup_A f)^{-1} \circ \rho \circ \psi^{-1})_* d\text{vol}_{S^3}$. By direct computation, one can show that $((f_1 \cup_A f)^{-1} \circ \rho \circ \psi^{-1})_* d\text{vol}_{S^3} = \frac{1}{2p} d\theta dx dy$, and so the final pdf is given by $p_1 \cup_A p_2(e^{i\theta}, x, y) = \frac{1}{2p} p_{V_1} \cup_A p_{V_2}(e^{i\theta}, x, y) = \frac{1}{2} p_{sym} \circ \psi \circ \iota \circ h_i^{-1}(e^{i\theta}, x, y)$ if $(e^{i\theta}, x, y) \in T_i$, where $p_1 \cup_A p_2$ is now a pdf with respect to $d\theta dx dy$.

A.2 Training Architecture Details

We train on each tori T_i separately with target q_i (q_i defined in 3.1). Recall that a trainable map on a torus is constructed as a sequence of coupling layers, with each coupling layer a function $\mathbb{R}^3 \rightarrow \mathbb{R}^3$. Formally, the layer keeping the coordinate corresponding to S^1 fixed is

$$c_1(y_1, y_2) = (y_1, y_2 \odot e^{s^1(y_1)} + t_1(y_1))$$

and, keeping the coordinates corresponding to D^2 fixed

$$c_2(y_1, y_2) = (y_1 e^{s_2(y_2)} + t_2(y_2), y_2)$$

Above, the s_i and t_i are trainable linear neural networks of appropriate size (either 2x1 or 1x2). Specifically:

$$s_i : \text{Linear}(i, \text{hdim} = 64) \rightarrow \text{ReLU} \rightarrow \text{Linear}(\text{hdim} = 64, i \pmod{2} + 1) \rightarrow \text{Tanh}$$

$$t_i : \text{Linear}(i, \text{hdim} = 64) \rightarrow \text{ReLU} \rightarrow \text{Linear}(\text{hdim} = 64, i \pmod{2} + 1)$$

Let $\psi : \mathbb{R}^2 \rightarrow \text{int}(D^2)$ be the diffeomorphism defined by $\psi(v) = \frac{v}{1+\|v\|}$. The forward diffeomorphism $F_\theta : S^1 \times D^2 \rightarrow S^1 \times D^2$ is therefore defined as:

$$(\theta, v) \mapsto (\theta, \psi(v)) \xrightarrow{c_1^1 c_2^1 \dots c_1^n c_2^n} (\theta_c, v_c) \mapsto (\theta_c \pmod{2\pi}, \psi^{-1}(v_c))$$

Let $F_{\theta_i} : Z_i \rightarrow T_i$ be defined as above where Z_i is equipped with the prior distribution μ_{Z_i} defined in 3.2, and T_i equipped with q_i defined in 3.1. The loss function used in training F_{θ_i} is:

$$L_i = \mathbb{E}_{z \sim \mu_{Z_i}} \left[\log(p_{Z_i}(z)) - \log(|\det J_{F_{\theta_i}}(z)|) - \log(q_i(F_{\theta_i}(z))) \right] - \beta_0 \max(0, 1 - t/T) H(F_{\theta_i*} \mu_{Z_i})$$

where $H(F_{\theta_i*} \mu_{Z_i})$ is the Shannon entropy of $F_{\theta_i*} \mu_{Z_i}$ given by

$$H(F_{\theta_i*} \mu_{Z_i}) = -\mathbb{E}_{z \sim \mu_{Z_i}} \left[\log(p_{Z_i}(z)) - \log(|\det J_{F_{\theta_i}}(z)|) \right]$$

In the equation of L_i , β_0 determines the total entropy contribution, t is the current epoch, and T determines the duration of additional entropy. Additionally, we note that all networks were initialized with biases set to 0 using orthogonal weights in the matrices, except for networks with output dimension ≤ 2 , which used uniform Xavier initialization with gain 0.01. These initializations gave smaller initial KL values and reduced the required number of training epochs to reach minimal KL values.

A.3 Post Training Metrics

Post training, along with local KL metrics on T_i , we also report global metrics on all of $T_1 \cup_A T_2$. Indeed, recall from 3.1, we expressed the target distribution as $X = (1 - X_B)X_1 + X_B X_2$. Let $F_{\theta_i} : Z_i \rightarrow T_i$ be the trained diffeomorphism and let $Y_i \sim \mu_{Z_i}$. Then $X \approx X_a = (1 - X_B)F_{\theta_1*}Y_1 + X_B F_{\theta_2*}Y_2 = (F_{\theta_1} \cup F_{\theta_2})_*((1 - X_B)Y_1 + X_B Y_2)$. Hence, the global KL divergence is given by:

$$\text{KL}(X_a | X) = \mathbb{E}_{z \sim (1-X_B)Y_1 + X_B Y_2} [\log(p_{X_a}(z)) - \log(q((F_{\theta_1} \cup F_{\theta_2})(z)))]$$

In the experimental results, we compute this by purely sampling X_a , but we still derive a relationship between the global metric and the local ones - thereby giving a way to verify

global sampling accuracy. Using the fact that both tori are disjoint almost everywhere, the law of total expectation, and canceling normalization constants, we have

$$\begin{aligned} \text{KL}(X_a|X) &= (1 - I_2)\mathbb{E}_{z \sim Y_1} \left[\log(p_{Z_1}(z)) - \log(|\det J_{F_{\theta_1}}(z)|) - \log(q_1(F_{\theta_1}(z))) \right] + \\ &\quad I_2\mathbb{E}_{z \sim Y_2} \left[\log(p_{Z_2}(z)) - \log(|\det J_{F_{\theta_2}}(z)|) - \log(q_2(F_{\theta_2}(z))) \right] \\ &= (1 - I_2)\text{KL}(F_{\theta_1*}Y_1|X_1) + I_2\text{KL}(F_{\theta_2*}Y_2|X_2) \end{aligned}$$

In other words, the total KL divergence is equal to the $(1 - I_2)$ times the KL divergence on T_1 summed with I_2 times the KL divergence on T_2 .

A.4 Potential Function

We provide a derivation of the Boltzmann distribution on S^3 associated to a Benzene molecule. Let $U(n, \phi; \kappa, c, V) = -\kappa(n \cdot c)^2 + (n \cdot c)^2 V(1 - \cos(6\phi))$. The first term is a Maier-Saupe potential which describes the interaction of Benzene and another molecule - $n \in S^2$ representing the normal vector to Benzene and $c \in S^2$ representing some molecular orientation vector of the other molecule. The second term is a 6-fold Hindered Rotor potential which describes the energy potential of Benzene associated to its angular configuration about the plane normal to c . We lift this energy potential to S^3 by acting via the unit quaternions $q \in S^3$, the lifted potential is given by:

$$U(q; \kappa, c, V, x_0, y_0) = -\kappa(n(q; x_0) \cdot c)^2 + (n(q; x_0) \cdot c)^2 V(1 - \cos(6\phi(q; y_0)))$$

where $x_0 \in S^2$ is the initial normal state and $y_0 \in S^2$ is the initial angular state. The final Boltzmann distribution is therefore given by

$$p_{S^3}^{\text{Boltz}} = \frac{1}{C} e^{U(q; \kappa, c, V, x_0, y_0)}$$

for some normalization constant C . We now define $n(q; x_0)$ and $\phi(q; y_0)$.

Given an element $q = (w, x, y, z) \in S^3$, we associate its element of $SO(3)$ given by:

$$R(q) = \begin{pmatrix} 1 - 2(y^2 + z^2) & 2(xy - wz) & 2(xz + wy) \\ 2(xy + wz) & 1 - 2(x^2 + z^2) & 2(yz - wx) \\ 2(xz - wy) & 2(yz + wx) & 1 - 2(x^2 + y^2) \end{pmatrix}$$

Then we define, as a function $S^3 \rightarrow S^2$

$$n(q; x_0) = R(q)x_0$$

Now, for $\phi(q; y_0)$, we require a bit more work. First, we rotate y_0 by $R(q)$ to obtain a vector $y_{\text{rot}} = R(q)y_0$. Let $\{e_2, e_3\}$ be an ordered basis for the plane normal to c . We project y_{rot} onto this ordered basis to obtain $y_{\text{rot}}^{\text{proj}} = m_2 e_2 + m_3 e_3$ and we define $\phi(q; y_0) = \text{atan2}(m_3, m_2)$.

In our setting, we restrict to $c = (1, 0, 0)$. Denote by $\{e_i\}_{i=1}^3$ the standard ordered \mathbb{R}^3 basis, so that $c = e_1$. We show that with this choice, the function U above is invariant under

the $L(12; 1)$ deck action on S^3 (see 2.2 for a definition in \mathbb{C}^2 coordinates). Indeed, if we let $g = e^{\frac{2\pi i}{12}}$ be a unit quaternion, then for any unit quaternion $q = w + xi + yj + zk \in S^3$, we have that $q \mapsto gq$ corresponds to the generating deck action in this representation. We verify first that the first term is invariant under $q \mapsto gq$. We see that $n(gq; x_0) \cdot e_1 = R(g)R(q)x_0 \cdot e_1 = R(q)x_0 \cdot R(g)^T e_1 = n(q; x_0) \cdot e_1$ where the last equality holds since $R(g)^T e_1 = e_1$ by direct computation, and so the first term is g invariant. Next, we do the second term. We note that, for $i \in \{2, 3\}$ $m_i = R(g)R(q)y_0 \cdot e_i = R(q)y_0 \cdot R(g)^{-1}e_i$ ie. these are the coefficients of projecting $R(q)y_0$ to the plane normal to e_1 but with new basis $\{R(g)^{-1}e_2, R(g)^{-1}e_3\}$. $R(g)^{-1}$ corresponds to fixing e_1 and rotating the y, z plane by $\frac{-\pi}{3}$. Therefore, $\phi(gq; y_0) = \phi(q; y_0) + \frac{\pi}{3}$ where equality is mod 2π . This shows that the second term is g -invariant due to factor of 6 in the cosine function.